College of Engineering
UNIVERSITY OF WISCONSIN–MADISON

Aerodynamics Final Project - Fall 2022

Nikolaj Hindsbo

Taught by
Professor Jennifer Franck

Abstract

This final project is a conclusion to the semester-long class of Aerodynamics. Included in this report is a 2D and 3D analysis of airfoils and wings and a comparison of methods to do so. The target audience of this report would be a student that has not taken aerodynamics, so so some things will be explained to a certain degree, but the derivations will be limited. Rather, there may be references to the book or in-class notes where the final step to the derivation is summarized. In this report, the Thin Airfoil Theory and Vortex Panel Method were derived for airfoils in a 2D analysis. Further mach number effects and Airfoil properties were explored as well as a discussion. Additionally, a 3D Analysis was done. This analysis included the Lifting Line Theory Elliptic Solution, Lifting Line Theory General Solution, a discussion of the two, and then a Taper XFLR ratio discussion. Finally, a wrap up with aspect ratio discussion.

Contents

1 2D Analysis

1.1 Thin Airfoil Theory

The class textbook - Fundamentals of Aerodynamics (FoA) Sixth Edition by John Anderson - will often be cited in this report. The first part of this assignment is to use the thin airfoil theory to compute the lift coefficient (C_l) as a function of α. To start, a derivation of thin airfoil theory is derived in FoA Chapter 4 Equation (4.57) to state the general airfoil coefficient of lift 1.

$$c_l = 2\pi(\alpha + \frac{1}{\pi}\int_0^\pi \frac{dz}{d\theta}(cos(\theta_0) - 1))d\theta_0) \tag{1}$$

Equation 1 states the general airfoil coefficient of lift for a NACA airfoil, where $\frac{dz}{d\theta}$ represents the slope of the camber line of an airfoil and α represents the angle of attack.

$$c_l = 2\pi(\alpha + \alpha_{L=0}) \tag{2}$$

Equation 2 also shows the more general way to do this analysis without a NACA airfoil. Reducing this is important because we will solve for the $\alpha_{L=0}$ term generally by computing the integral term in Equation 1. The general equation for the slope of a NACA airfoil camber line can be defined mathematically as well, as explained in class notes [1].

$$\begin{aligned} \frac{dz_c}{dx} &= \frac{2M}{p^2}(p - x) \mapsto 0 \leq x < \theta_p \\ \frac{dz_c}{dx} &= \frac{2M}{(1-p)^2}(p - x) \mapsto \theta_p \leq x < \pi \end{aligned} \tag{3}$$

Then, mapping of x = $\frac{1-cos(\theta_0)}{2}$ and combining Equations 1 - 3 simplifies the result.

$$\alpha_{L=0} = \frac{m}{4\pi p^2(p-1)^2}[(8p-6)(\pi p^2 - 2p\theta_p + \theta_p) + 8(2p^2 - 3p + 1)sin(\theta_p) + (2p-1)sin(2\theta_p)] \tag{4}$$

Where the constants p, m, and θ_p can be described using the numbers of a NACA foil (e.g. NACA #1#2#3#4).

$$
\begin{aligned}
m &= \frac{\#1}{100} \\
p &= \frac{\#2}{10} \\
\theta_p &= arccos(-2p+1)
\end{aligned}
\tag{5}
$$

For the NACA 2412 airfoil, using these values for Equation 5 into 4 , this gives a value $\alpha_{L=0}$ = -0.0363. Therefore, the thin airfoil theory for the NACA 2412 predicts the coefficient of lift as a function of α to be:

$$
c_l = 2\pi(\alpha + 0.0363) \tag{6}
$$

This distribution was also plotted.

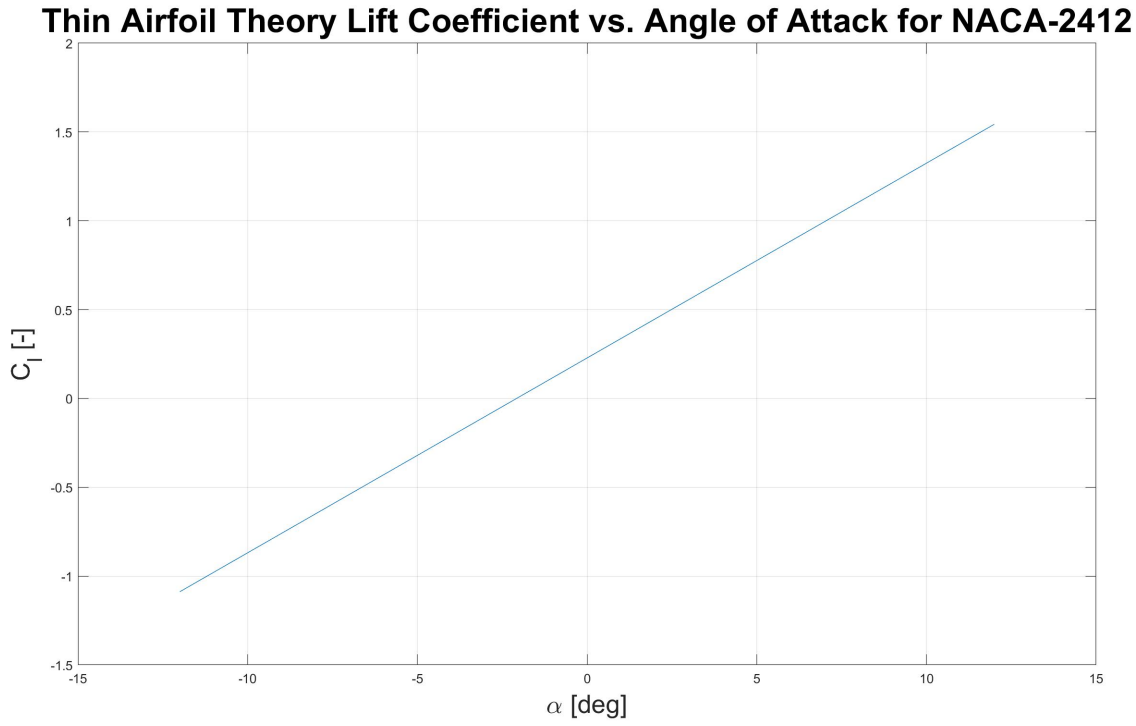

Figure 1: Plot of the Thin Airfoil Coefficient of Lift as a Function of α.

Figure 1 shows the coefficient of lift of the NACA 2412 2D airfoil as a function of α as predicted by the thin airfoil theory.

1.2 Vortex Panel Method

The Vortex Panel l modeling strategy, limitations, and comparisons will come in part 1D. What a reader should briefly know is that the vortex panel uses a panel technique directly analogous to the source panel method, however, a vortex has circulation unlike the source so it is useful in lifting cases. The vortex panel method allows us to derive lift from the geometry of an airfoil.

In homework 9, the vortex panel method was derived. The summary of it is that there is a contribution of n panels to a potential at the control point of the ith panel, a normal component of velocity equal to zero, and the velocity is the superposition of uniform flow velocity and velocity induced by all the vortex panels. Using this, the crux of vortex panel method was derived in textbook Equation 4.79 [2].

$$V_\infty cos(\beta_i) - \sum_{j=1}^{n} \frac{\gamma_i}{2\pi} J_{i,j} = 0 \tag{7}$$

This is just the basis - the actual nonlinear pattern vortex panel method that is more accurate was derived in supplemental notes given in class [1]. The integrals depend on the panel geometry, not the flow, and integrated for all the number of panels. In my vortex panel method, I normalized the flow such that the chord length was 1 unit meter and the freestream velocity was 1 m/s. The number of panels used in this analysis was 140. In addition to the n equations, the flow must also satisfy the Kutta Condition. The code of my matlab code is very well commented, so one can follow it in the submitted Matlab code files for this submission for all the A,B,C, etc. constants that go into the vortex panel method. The full explanation of the Vortex Panel Method was provided with in-class supplemental notes [1].

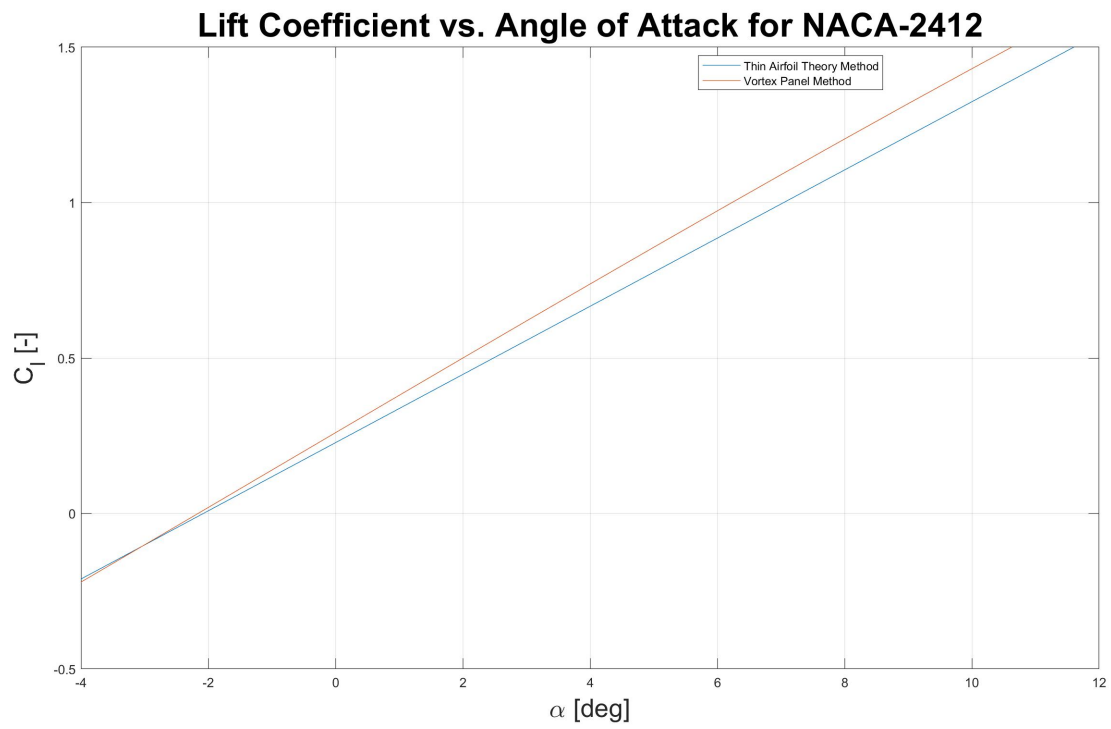

Figure 2: Plot of Coefficient of Lift as a Function of α for Thin Airfoil and Vortex Panel Method.

As seen in Figure 2, the coefficient of lift as a function of α predicted for the thin airfoil theory and vortex panel method are actually a bit different.

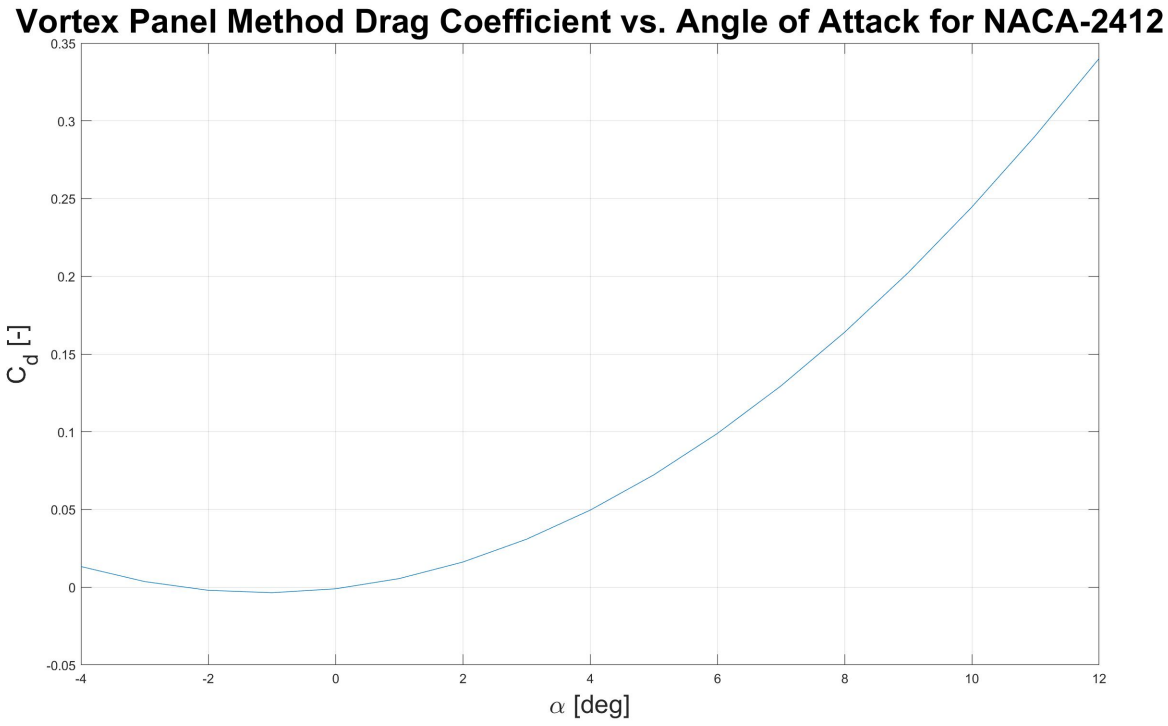

Figure 3: Plot of Coefficient of Drag as a Function of α for the Vortex Panel Method.

The next step for the Vortex Panel Method report was also getting the coefficient of drag for the NACA2412 airfoil as a function of α. One can obtain the coefficient of drag with the same methodology as lift with the vortex panel method except for that the drag is the component of the pressure along the panel that is in the horizontal direction.

1.3 XFLR5 Data

The next step in this report is XFLR5 data. As with the previous subsections, there will be a discussion of and between method used in more detail in the next subsection. To get airfoil data based on the XFOIL method, the XFLR5 software was used for all analyses in this report involving XFOIL derived data. Then, the analyzed data was exported to Matlab for visualization purposes.

To start of, download the XFLR5 software. Then, create a new project and import the desired NACA Airfoil. To create an airfoil, select File –> Direct Foil Design. XFLR5 automatically generates airfoil profiles for NACA 4 and 5-series airfoils. To do this, select Foil –> Naca Foils. Enter the foil number and the desired number of panels. For this, I used the digits 2412 and Number of Panels 200. Additional accuracy comes with more panels. Then, to start an analysis on a NACA Airfoil one must use Analysis –> Define an Analysis. Importantly, the Reynold's number and Mach Number should be defined. Thus far, Mach number has not been a concern and it is okay to leave that at zero. However, Reynold's number is important. Since everything is normalized (chord length of 1, $V_\infty = 1$, and the airfoil is in air), I solved for the airfoil to have a Reynold's number of approximately 67,000. Sometimes these airfoils may have troubles converging and a possible solution is to change the Reynold's number. This is what happened with mine in an upcoming section, so I set Re = 68,000 for this analysis to stay consistent and close to the Thin Airfoil and Vortex Panel Methods.

When the Reynold's number is defined, press OK and a new pane labled "Direct foil analysis" should appear. Here, set the anlysis setting for a function of α, check the sequence, and I used start = -4 degrees, end = 12 degrees, and delta = 0.5 degrees. Check all boxes above analyze. When ready, run the analyze button to get started. As previously mentioned, it is someitmes important to change Reynold's number or Mach number justifiably if the series is unable to converge. To show results, right click the software and select "show all polars" or right-click an analysis in the Object Explorer tab to export the data into a CSV.

For the NACA2412 airfoil, this subsection will compare the results of c_l and c_d as a function

of α to the Thin Airfoil Theory and Vortex Panel Methods.

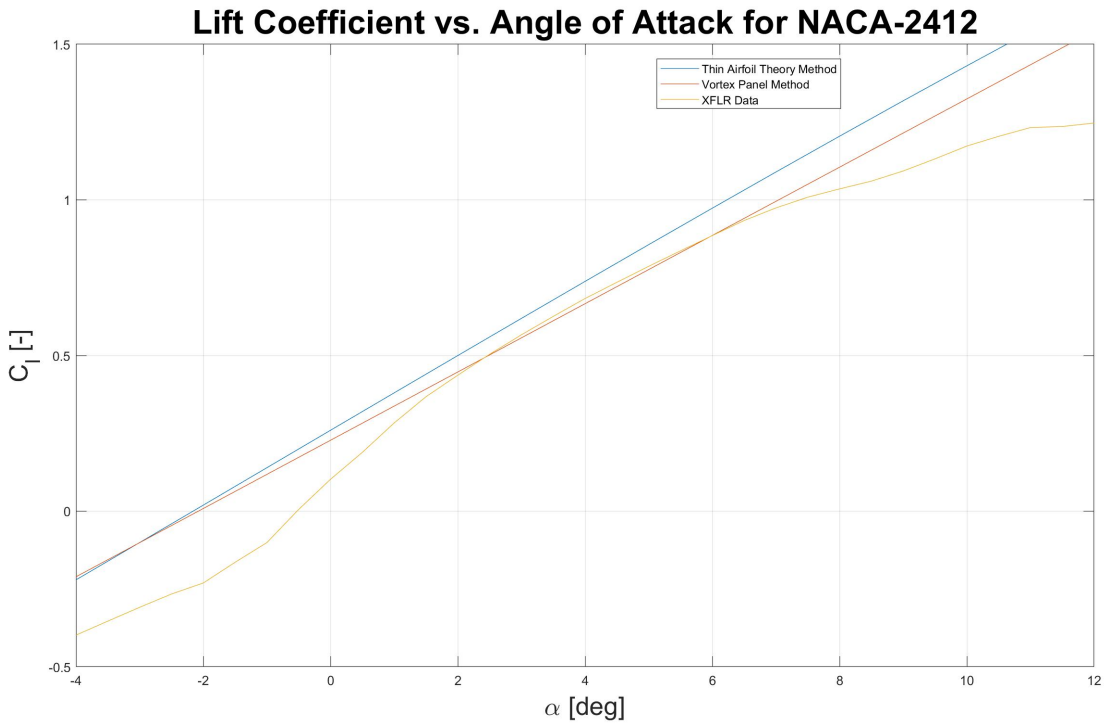

Figure 4: Plot of Coefficient of Lift as a Function of α for all three methods.

Firstly, the coefficient of lift. When comparing these three methods, it is very interesting to note that while the VP and Thin Airfoil methods remain linear in pattern, the XFLR5 data is clearly not. More will be talked about this in the discussions Subsection 1.4.

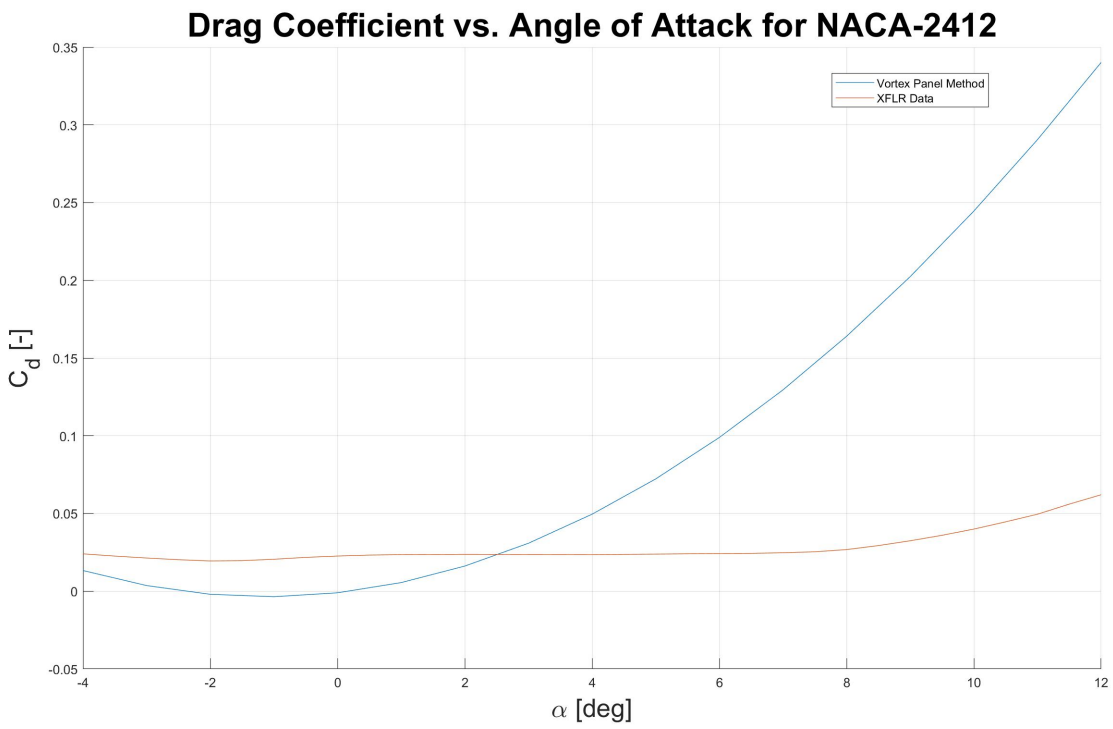

Figure 5: Plot of Coefficient of Drag as a Function of α for XFLR and Vortex Panel Method.

Additionally, the coefficient of lift for the Vortex Panel Method and XFLR5 Data. When comparing the two methods, they do not seem to agree at all. More will be talked about this in the discussions Subsection 1.4, but the XFLR5 XFOIL method limitation that is often talked about is its under-estimation of drag [3].

1.4 Discussion Points - Methods of 2D Analysis

Discussion of the Thin Airfoil Theory, Vortex Panel Method, and XFLR data likeness and differences in reference to the Coefficient of Lift and Drag covered in the previous subsections will begin here now.

Firstly, the Thin Airfoil Theory. Subsection 1.1. The Thin Airfoil Theory starts at the most basic case - a thin, symmetric airfoil. Then, the cambered solution to this (which was the one ultimately used in 1.1) is derived from this. The thin airfoil theory says that a *thin* airfoil (t/c $<$ 0.12) airfoil can be simulated by a vortex sheet placed along the camber line. The purpose is to calculate the variation of $\gamma(s)$ and enforce the Kutta Condition on the trailing edge. Then, lift can be calculated from circulation via the Kutta-Joukowski Theorem. Another condition that is important in the Thin Airfoil Theory is that the should be no flow *normal* to the surface of the airfoil [2]. The fundamental airfoil theory simply states - the camber line is a streamline

of the flow. The most important result from the Thin Airfoil Theory is that it predicts that the theoretical result of lift coefficient is *linearly proportional to angle of attack*. It also states that the theoretical lift coefficient for c_l vs α is $2\pi[1/rad]$. However, the expression for c_l itself differs between a symmetric and cambered airfoil because there exists a angle of zero lift that is a negative value.

The Thin Airfoil Theory results from Section 1.1 are as expected. The coefficient of lift as a function of angle of attack is a straight line equation that has a negative angle of zero lift. Although they are expected, there are definitely limitations to the thin airfoil theory. Firstly, the thin airfoil has two main assumptions: the airfoil is significantly thin and the angle of attack must be low (works best when aoa < 12). When comparing to experimental data, the Thin Airfoil theory actually performs quite well if these assumptions hold true. A comparison was done to compared to the experimental data of the NACA 2412 airfoil provided in class notes [1]. For the low angles of attack, the distribution of coefficient of lift versus angle of attack was very linear with a slope approximately that predicted from the Thin Airfoil Theory. Additionally, the angle of zero lift was extremely close to the experimental. *However,* the model and experiments start to fall off in higher angles of attack because the airfoil starts to experience stall and the linear pattern is disrupted. The thin airfoil theory does not account for this. Additionally, the thin airfoil theory does not provide a great fit for sufficiently thick or odd-shaped foils because their pattern of lift versus alpha does not follow the slope of 2 $\pi[1/rad]$. Obviously, not all airfoils are thin, so the Thin Airfoil Theory does not account for this, but many airfoils we deal with are so it is a great method [2]! Overall, I would not improve this model because its simplicity is the charm of it. Instead, it is important to realize the limitations of the thin airfoil theory and make sure they hold true in your analysis.

Secondly, the Vortex Panel Method, Subsection 1.2. The biggest difference between the Vortex Panel Method and the Thin Airfoil Theory is that the Vortex Panel method allows us to be concerned with the generation of aerodynamic lift and drag on other body shapes of arbitrary thickness, shape, and orientation. We are solving the coefficient of lift as a function of the *geometry* of the airfoil instead of its angle of attack properties! Specifically, it is a numerical technique that is analogous to the Source Panel Method, except it uses vortices which generate circulation and thus lift. However, all n equations must satisfy the Kutta Condition - so we have a system of n equations with n unknowns. By covering the body surface with a vortex sheet along the complete surface of the body - such that that body surface becomes a streamline - we

develop a very accurate solution which can improve in accuracy with a greater number of panels.

Now, the results from Subsection 1.2 are as expected. The slope of the line is no longer exactly $2\pi[rad^{-}1]$, which we wouldn't expect for a Vortex Panel Method of the NACA 2412 airfoil. This is now closer to the experimental data along the line. However, the limitation of large angles of attack and stall are still present for the Vortex Panel Method and another limitation would be time - it takes significant time to set up a Vortex Panel Method for a slight increase in accuracy. Again, stall causes this a discrepancy between the VP method and experimental data - something that is not easily modeled. Therefore, it is also important to realize the limtations of the Vortex Panel Method - low values of alpha and a significant number of panels should be used for greater accuracy. Furthermore, viscous effects control drag at high angles of attack or Reynold's Number. Since there would be seperation on a real airfoil (which is not accounted for in the Vortex Panel Method), this results in lower pressure along the boundary layer and furthermore actually lower lift and drag than the theory predicts. This is a key reason why the Vortex Panel Method differs both experimentally and from the XFLR data. You could improve the Vortex Panel Method by coupling it with an integral boundary layer equation to calculate more accurate aerodynamic properties of the airfoil.

Finally, the XFoil Method using XFLR5. XFLR5 uses underlying code of the XFoil Method. XFoil is also a panel-based method that uses the full potential methods to calculate flows around the two-dimensional airfoil sections. Unlike the Vortex Panel Method, it uses the presence of the boundary layer to create greater accuracy that is closer to what happens in the real world! The code deals with viscous analysis of airfoils, transition, bubbles, limited TE separation, and lift and drag predictions that are allow it to be more accurate than the Vortex Panel Method and Thin Airfoil Method solutions. However, XFoil also suffers some limitations from stall. As a airfoil starts to stall - the separation of boundary layers exists and the panel code becomes less reliable. This is the fundamental limitation of the code [4]. Despite this, the XFOIL method is highly accurate and at least show that stall is starting to become evident with its nonlinear response as the angle of attack increases (unlike the other two methods that do not show this pattern at all). It is extremely hard to make accurate measurements on airfoils with Low Reynold's Number (something that XFOIL is designed for), so it is a great tool to use.

Especially limiting it the XFOIL"s prediction of drag - it normally under predicts drag. This was also seen in Subsection 1.3 where the Vortex Panel Method better found drag. This is because there is a strong influence of laminar separation bubble on real airfoils - which doubles the drag

coefficient [3]. XFOIL takes this into account, but still underestimates the drag. Perhaps, XFOIL could be improved to conditionally check experimental values for drag and attempt to correct the assumptions they make. After all, all mathematical models have room for improvement - they all operate under a certain set of conditions that account for some aspects but may forget others that can happen in real life.

1.5 Mach Number Effect

In this part of the report, a compressible correction factor was applied to show how Mach Number affects the coefficient of lift for both the Vortex Panel Method and the XFLR5 data. As is widely known, the coefficient of lift of an airfoil will significantly change based on speed of the freestream velocity. One way to characterize velocity is using a Mach Number (M) - a comparison of the relative speed of the freestream velocity to the speed of sound (c).

$$M = \frac{V_\infty}{c} \tag{8}$$

Our methods work best in the subsonic region when Mach is <0.85 [2] - a region where the flow is still compressible and subsonic. In this comparison, we will show how the coefficient of lift distribution can be corrected for the Vortex Panel Method with a Mach Number of 0.1, 0.4, and 0.7. Simply, the coefficient of lift distribution derived in subsection 1.2 can be corrected using the the Prandtl-Glauert Rule to be more accurate [1].

$$C_l = \frac{C_{l,o}}{\sqrt{1 - M^2}} \tag{9}$$

Equation 9 states the Prandtl-Glauert correction rule to account for mach number of the infinite stream. For the Vortex Panel Method correction, $C_{l,o}$ represents the results from the Vortex Panel Method, C_l represents the corrected coefficient of lift, and M represents the Mach number of the flow.

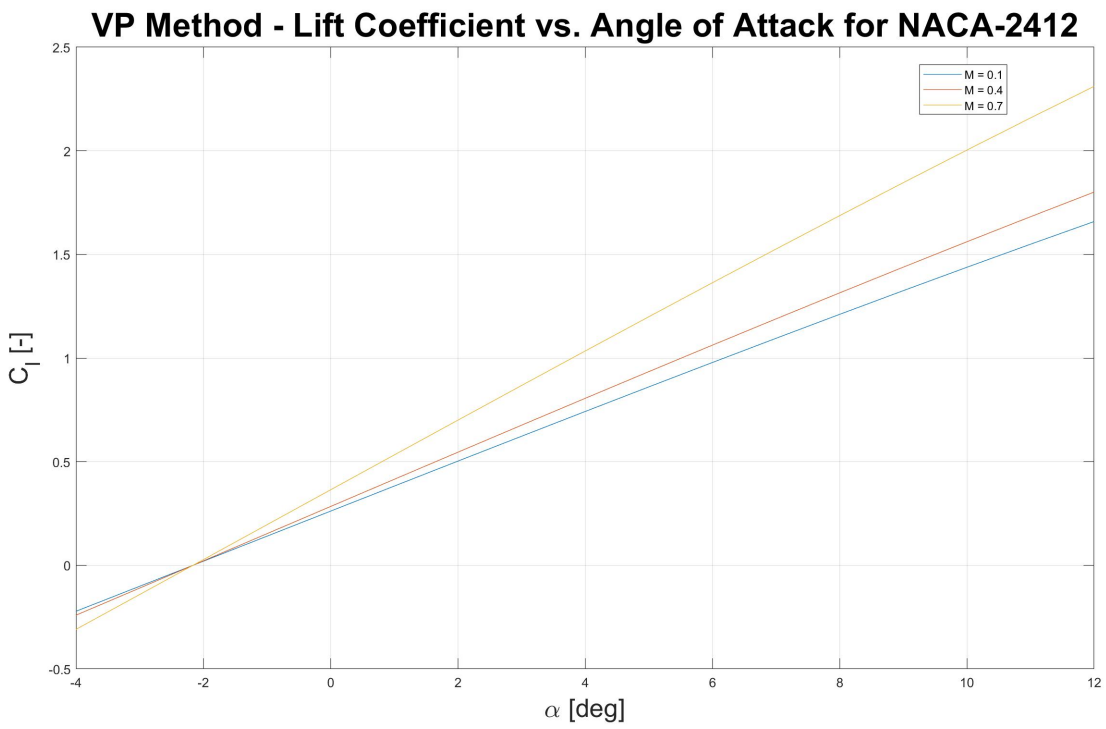

Figure 6: Coefficient of Lift as a Function of α at three distinct Mach Numbers for the VP Method.

Then, using our data of α vs. C_l from subsection 1.2 and using Equation 9 in Matlab, the distribution of the corrected coefficient of lift at different mach numbers was found. The legend in Figure 13 labels the Mach Number of the lines.

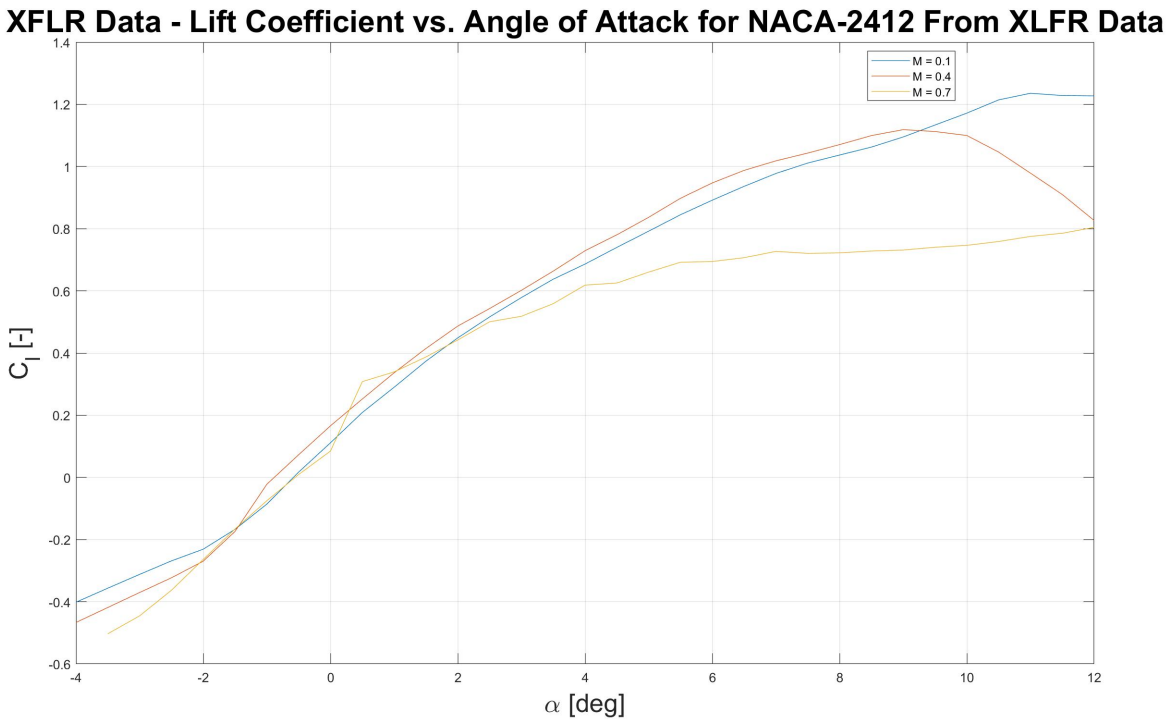

Figure 7: Coefficient of Lift as a Function of α at three distinct Mach Numbers for the XFLR Method.

Using the XFLR5 software, the lift distribution for the correction factor of the XFLR was also found. To replicate this, use the same analysis technique described in subsection 1.3 for the XFLR data. However, you will have to define three different analyses - one for each Mach Number and analyze all three separately. The, I exported all separately and analyzed data from an excel worksheet. Some errors could happen when trying to converge using the XFLR5 software. To avoid this, try a different Reynold's number. For the data provided in Figure 15 were all performed at Re = 68,000 and it was able to converge on all aoa except for -4 degrees for Mach number of 0.7.

1.6 Discussion Points - Mach Number Effect

As explained in subsection 1.4, the XFOIL algorithm does not use quite the same approach as the Vortex Panel method. As the Mach number increases, so does the separation of the boundary layer as the flow starts to approach the transonic

1.7 Airfoil Properties

In this section, I already have NACA 2412, so I chose 4424 as one of my foils because it has extreme thickness but is mostly similar to the 2412 in distribution, and I wanted to see if the Vortex Panel Method performed just as well on this foil. I also chose the 4412 airfoil because it was about half as thick at the same location with the same max camber. Both foils had max thickness at 30 percent of the chord and max camber of 4 percent at 40 percent the chord length. However, the thickness was about 2x as much for the 4424 compared to the 4412. Also, the 4412 is almost the same as NACA2412, except the max camber is twice as much on the 4412.

A summary of the 2412 Foil:

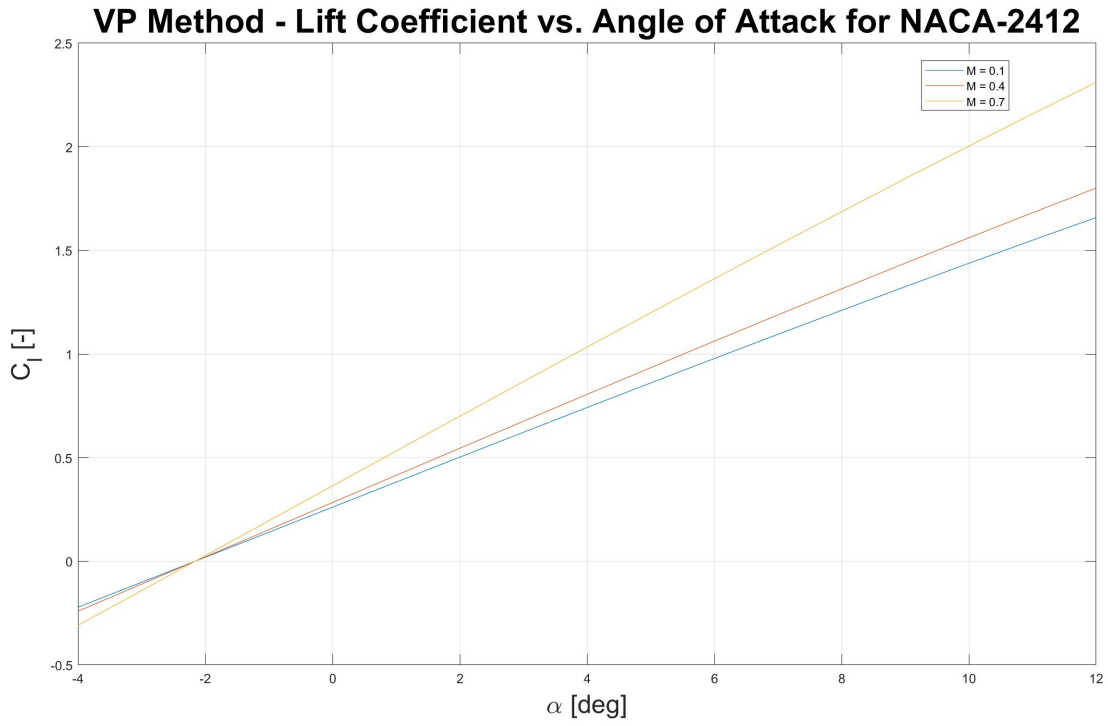

Figure 8: NACA 2412 Coefficient of Lift as a Function of α at three distinct Mach Numbers for the VP Method.

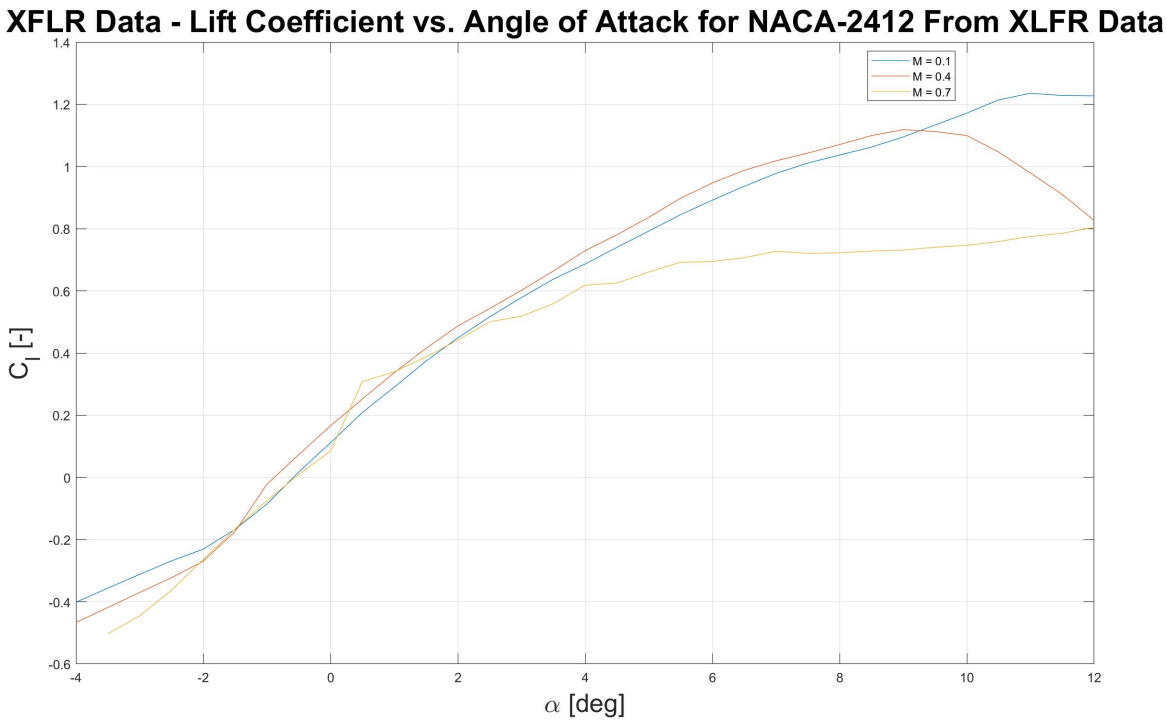

Figure 9: NACA 2412 Coefficient of Lift as a Function of α at three distinct Mach Numbers for the VP Method.

Firstly, the 4424 foil:

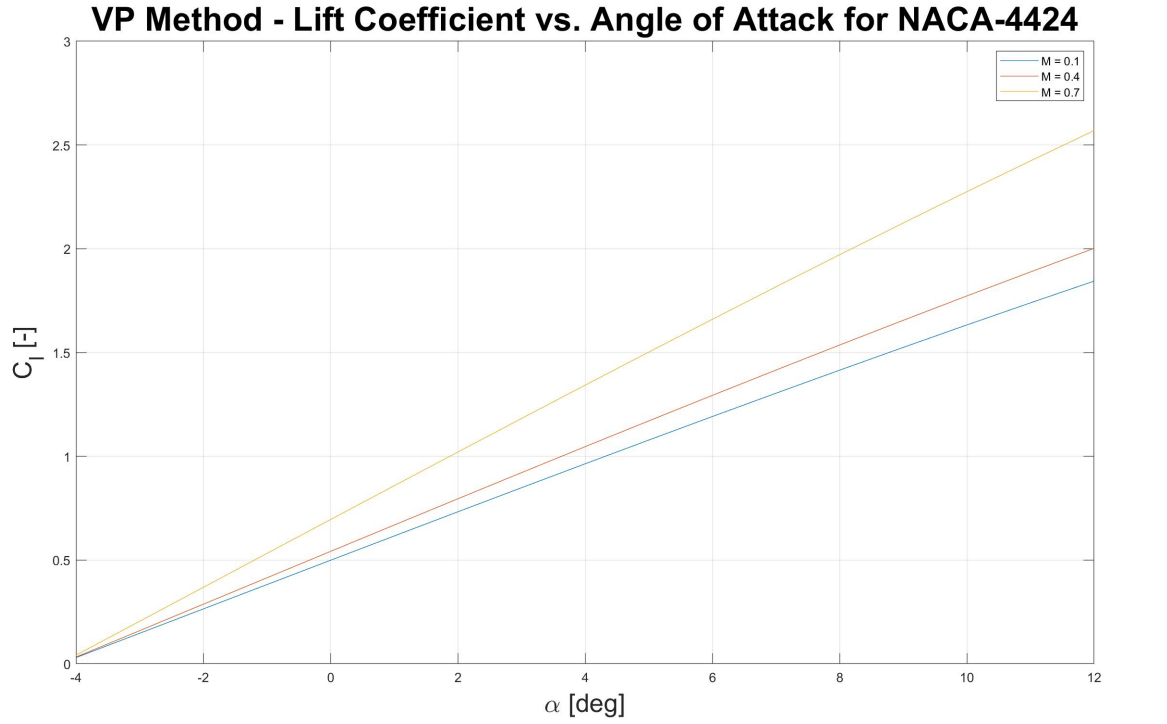

Figure 10: NACA 4424 Coefficient of Lift as a Function of α at three distinct Mach Numbers for the VP Method.

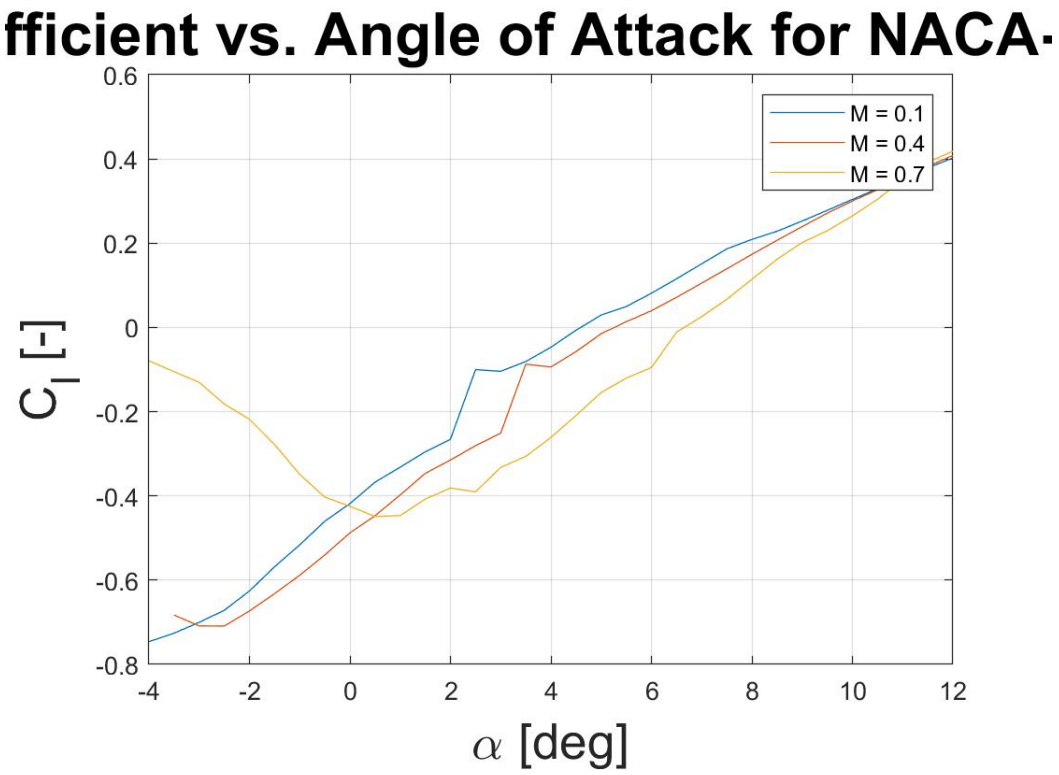

Figure 11: NACA 4424 Coefficient of Lift as a Function of α at three distinct Mach Numbers for the XFLR Method.

Compared to the 2412 foil, this distribution shows there may be limits to the vortex panel method as well! The XFLR data and vortex panel method varied significantly. Indeed, the huge thickness also changed the angle of zero lift to be lower than 4 degrees, almost double the amount of the 2412 airfoil!

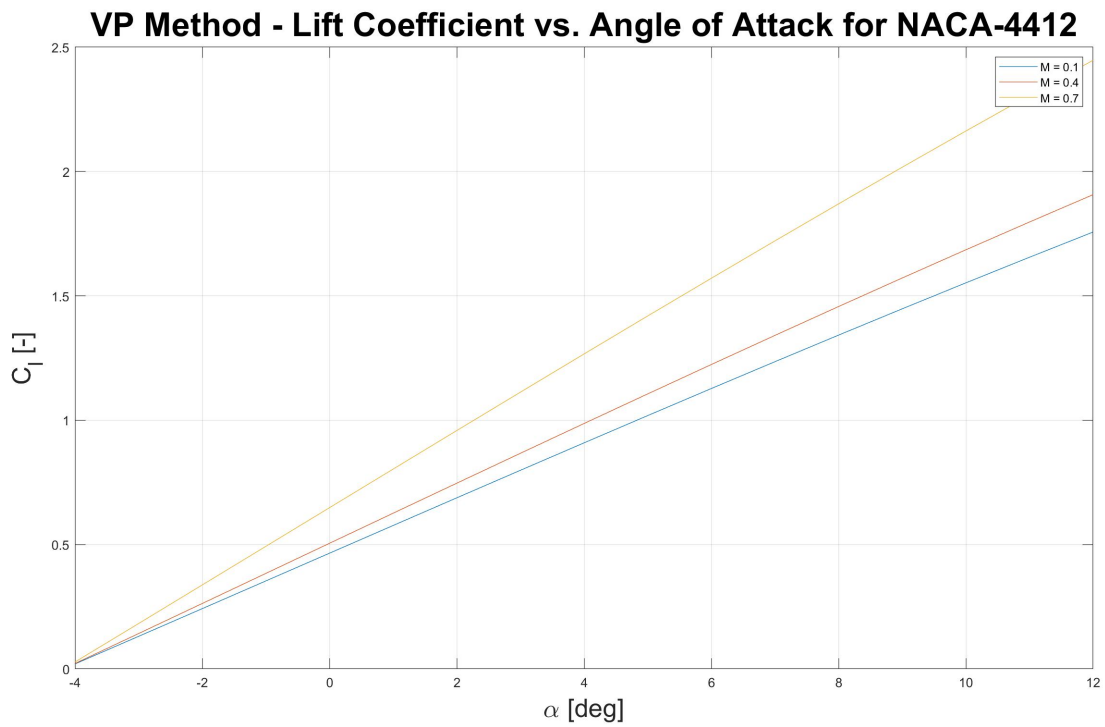

Figure 12: NACA 4412 Coefficient of Lift as a Function of α at three distinct Mach Numbers for the VP Method.

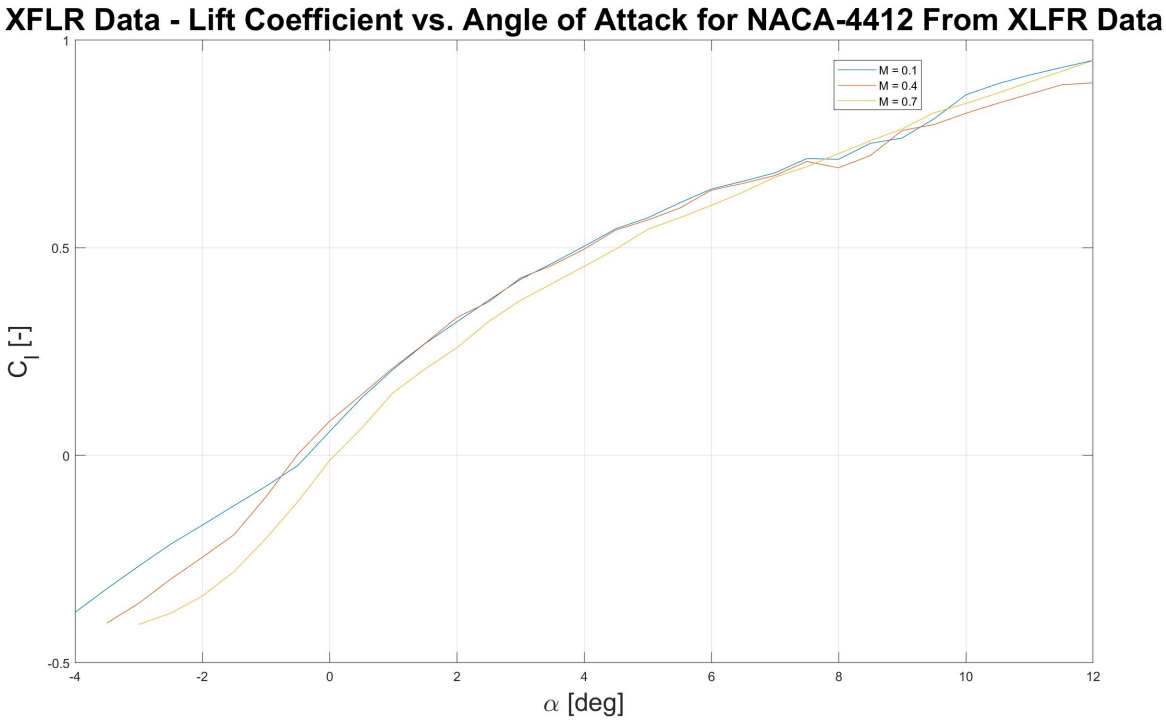

Figure 13: NACA 4412 Coefficient of Lift as a Function of α at three distinct Mach Numbers for the VP Method.

Very interesting! For the NACA 4412 foil, the angle of attack was the same (as predicted by the VP method) as the 4424 airfoil. However, the VP method for both of these methods overestimated the coefficient of lift extremely when compared to the XFLR data. It is worth noting that the NACA 4412 and 4424 airfoils were not able to converge at the same Reynold's number as theory, so there may be a difference there, but I was not expecting the results to differ by so much. Also, interestingly, these XFLR data appeared to be very unstable for this large thickness at large mach numbers - versus the 2412 that was both symmetric, decently thin, and not too cambered. Meanwhile, the thick foils seem to have a lesser coefficient of lift, but a larger alpha lift = 0.

2 3D Analysis

2.1 Lifting Line Theory Elliptic Solution

In this part of the report, we are interested in using the Lifting Line Theory described in Chapter 5 of the Aerodynamics Book [2]. The lifting theory was the first pratcial method of predicting aerodynamic properties for a finite wing and was developed by Ludwig Prandtl and his colleagues [2]. It lays the groundwork for modern numerical methods described in Chapter 5 [2]. Using concepts of down-wash, finite number of vertices, and the *lifting line*, we can obtain a great model for predicting 3D Lift of a wing. The fundamental equation of Prandtl's lifting-line theory is summarized in Equation 5.23 in the Aerodynamics book [2]. This can be furtehr simplified for an elliptic lift distribution because the downwash is *constant* over the span for an elliptical lift distribution [2]. There are a few fundamental ideas for an elliptical distribution that carry out the analysis.

$$\alpha_i = \frac{\Gamma_0}{2bV_\infty} \tag{10}$$

This conclusion results in an induced angle being constant along the span of an elliptic lift distribution.

$$\Gamma(y) = \Gamma_0 \sqrt{1 - \frac{2y}{b}^2} \tag{11}$$

Equation 11 is the elliptical circulation distribution of an elliptical lift distribution wing along its span.

$$\alpha = \frac{\Gamma_0}{\pi V_\infty} c + \alpha_{L=0} + \frac{\Gamma_0}{2bV_{inf}} \tag{12}$$

Therefore, combining Equation 11 to Prandtl's General Fundamental Solution in 5.23 [**?**], we can get the circulation as a function of alpha. In equation 16.

However, we have three unknowns currently. Γ_0, $\alpha_{L=0}$, and c, the chord length. Firstly, this is a symmetric foil - so $\alpha_{L=0}$ drops to zero [1]. Also, since this is an elliptical distribution with known AR = 6, we know the chord length as a function of y.

$$c(y) = b/6\sqrt{1 - (2y/b)^2)} \tag{13}$$

Equation 13 represents the chord distribution of an elliptic distribution as a function of y [2].

$$\frac{\Gamma(y)}{2bV_\infty} = \frac{\alpha}{\frac{12}{\pi\sqrt{1-(2y/b)^2}+1}} * \sqrt{1 - (2y/b)^2} \tag{14}$$

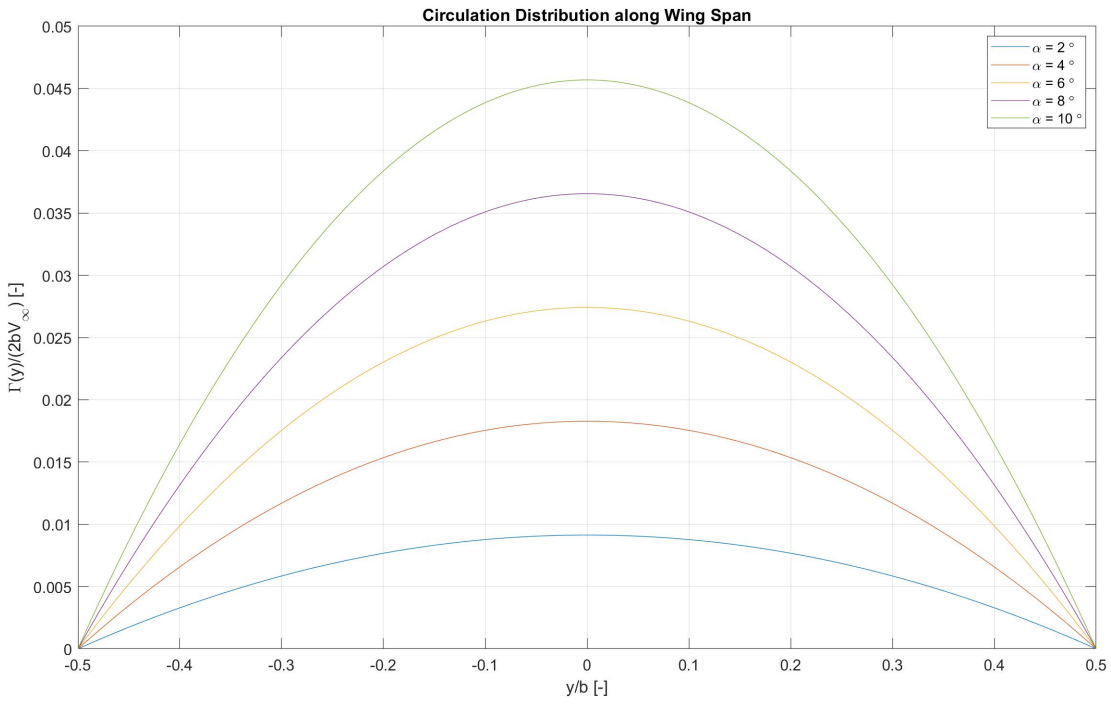

Figure 14: Normalized Circulation along the Wingspan of the Elliptical Wing

Therefore, combining Equations 11 - 13, the equation for gamma distribution as a function of span (y) was obtained and plotted in Matlab for the values α = [2, 4, 6, 8, 10] degrees. As seen,

the circulation increases as the angle of attack increases and is maximized in the middle of the span of the wing where circulation is greatest as predicted by the lifting line theory.

Additionally, the coefficient of lift and drag were asked to be found for this elliptic wing.

$$\alpha_i = \frac{C_L}{\pi AR} \tag{15}$$

The book shows that the induced angle of attack can be simplified as a function of the coefficient of lift (C_L) and the aspect ratio. The, using the relation between circulation distribution in 10 and Equation 11 for the distribution of circulation, one can find an equation for C_L because Γ_0 is found as the maximum value from 11 [2].

$$\Gamma_{y=0} = \frac{C_L}{\pi AR} \tag{16}$$

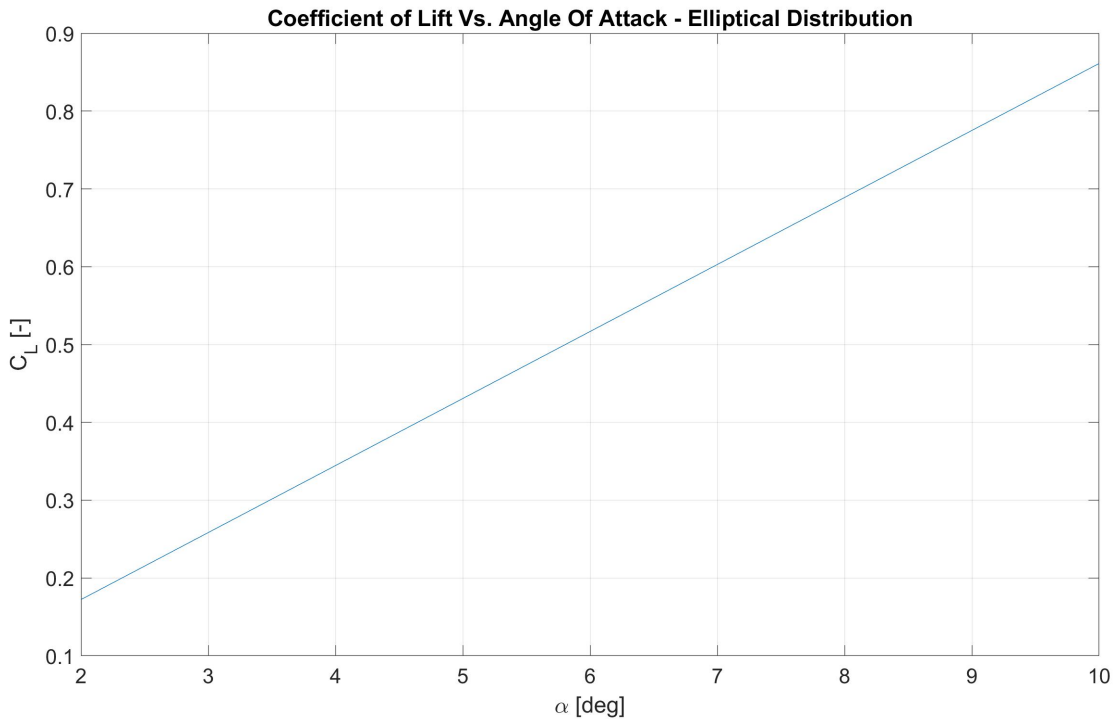

Figure 15: Coefficient of Lift vs. AoA for Elliptical Distribution

s

$$C_{D,i} = \frac{C_L^2}{\pi AR} \tag{17}$$

Likewise, Equation 5.43 in the book relates the Coefficient of Induced Drag to the lift distribution. This is summarized in Equation 17

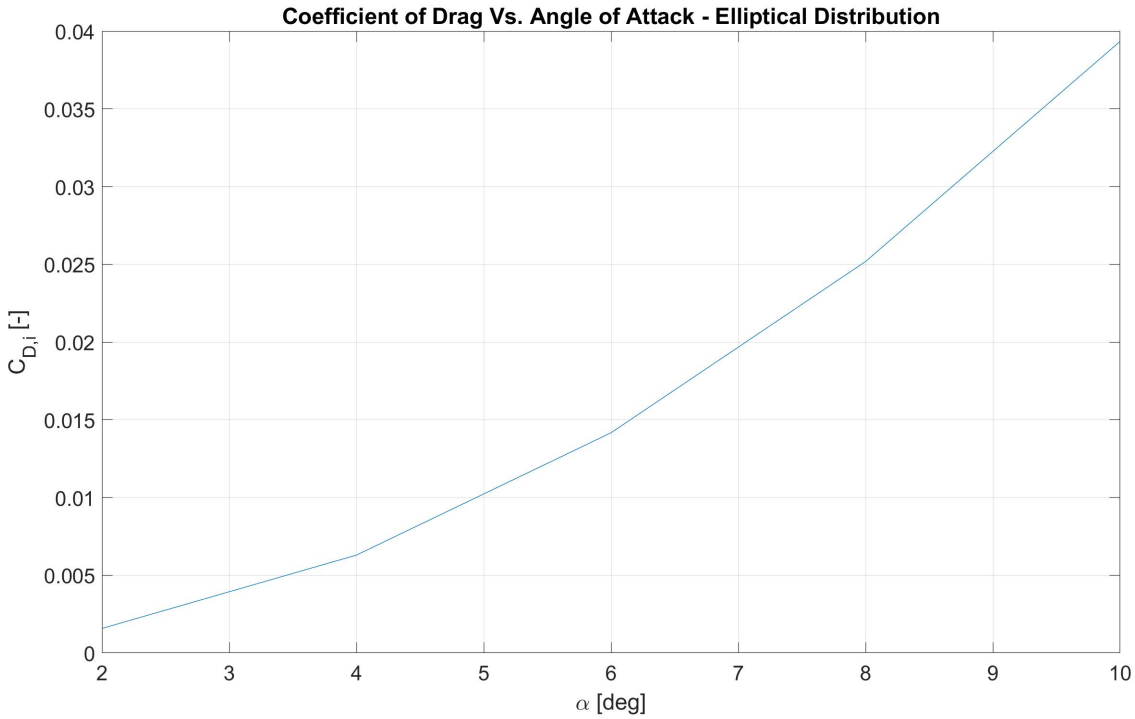

Figure 16: Coefficient of Drag vs. AoA for Elliptical Distribution

Figure 16 shows the coefficient of drag vs. AoA for the elliptical distribution. As expected, it is a nonlinear-ish distribution of the linear-ish coefficient of lift.

2.2 Lifting Line Theory General Solution

Next is the Lifting Line Theory General Solution. In this part, I used Matlab to calculate the A_n coefficients of each Fourier sine series with 2-16 terms.

For a wing with a constant chord length, the Aspect Ratio (AR) can be summarized as AR = b/c. From the book, the Fourier sine series that is expanded simplifies to Equation 5.51 [2].

$$\alpha(\theta_0) = \frac{2AR}{\pi} \sum_{1}^{N} A_n sin(n\theta_0) + \alpha_{L=0}(\theta_0) + \sum_{1}^{N} sin(\frac{n\theta_0}{sin(\theta_0)}) \tag{18}$$

For a symmetric airfoil the $\alpha_{L=0}$ term drops to zero, and Equation 18 simplifies. To sum in Matlab, you can "simply" do a nested loop for N = 2-16 Fourier transforms using Equation 18. Then, we are interested in plotting along y/b 0–> 1. Using Equation 5.46 from the book, we transform y to polar.

The bounds of Equation **??** are described as θ 0 –> 1. However, solving for Equation 18 result in const/0 for the ends, so you must go from 0.01 —> .99 π to avoid this in your code.

In order to plot $\frac{A_N}{\alpha}$ as a function of N you can take 18 and divide out A_n to the other side (that is, you will be solving for just the sin terms. Then, set the Fourier transform = 1 on the LHS (because you have alpha/An on the LHS side, and you are plotting as a function of that magnitude) to solve for this coefficient and solve the N system of equations for N unknowns.

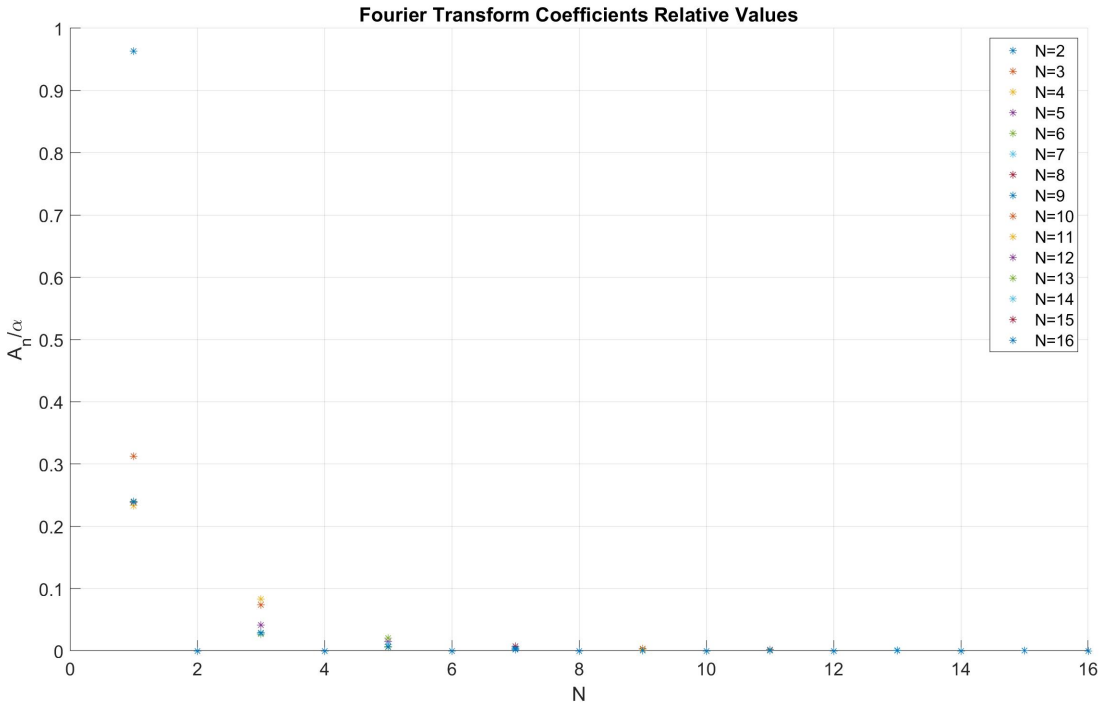

Figure 17: A_n distribution as a function of N 2-16

The distribution of circulation can similarly be found using the already existing numbers from the previous distribution. This general case is described in Equation 5.48 in the book [2]. Then transform y/b to theta using Equation 5.46.

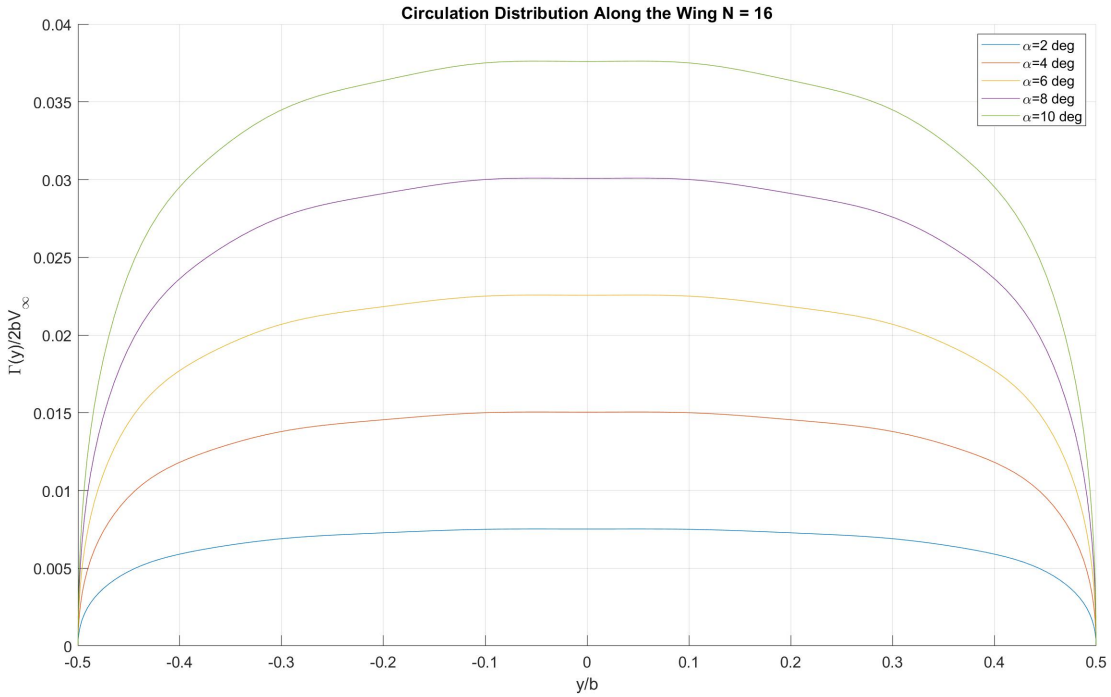

Figure 18: Circulation along the wing at alpha = 2-10 for N = 16

The resulting circulation distribution for N = 16 was found.

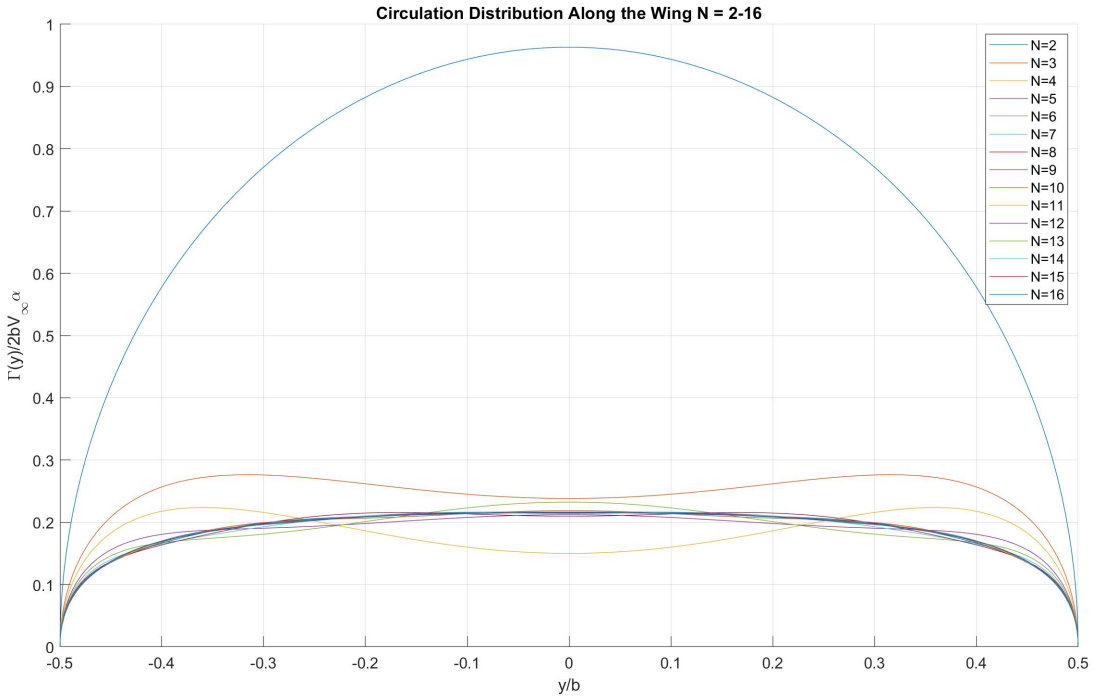

Figure 19: Circulation along the wing at alpha = 2-10 for N = 2-16

The resulting circulation for N = 2-16 can be seen in Figure 19. Using Equations 5.53 and 5.61 in the book, we can calculate Coefficient of Lift as a function of Angle of Attack [2].

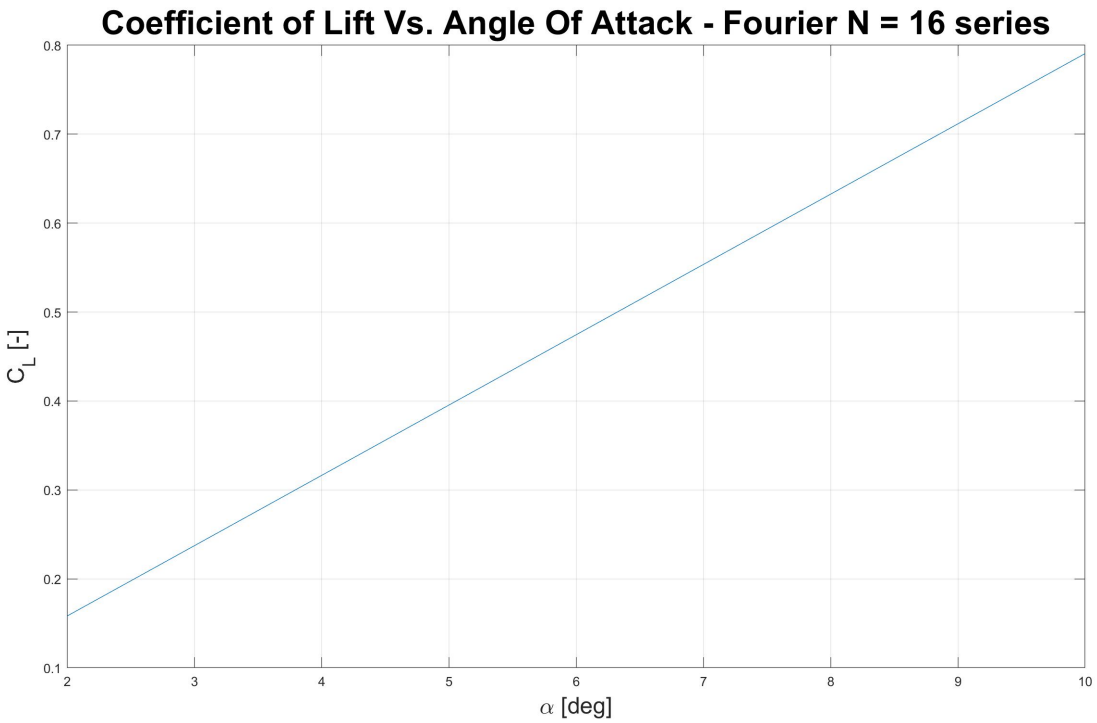

Figure 20: Coefficient of Lift vs. Angle of Attack for the Fourier N = 16 series for AR = 6

Still, the coefficient of lift follows a linear pattern between angles 2-10 for a 3D curve just like analysis done in part 1!

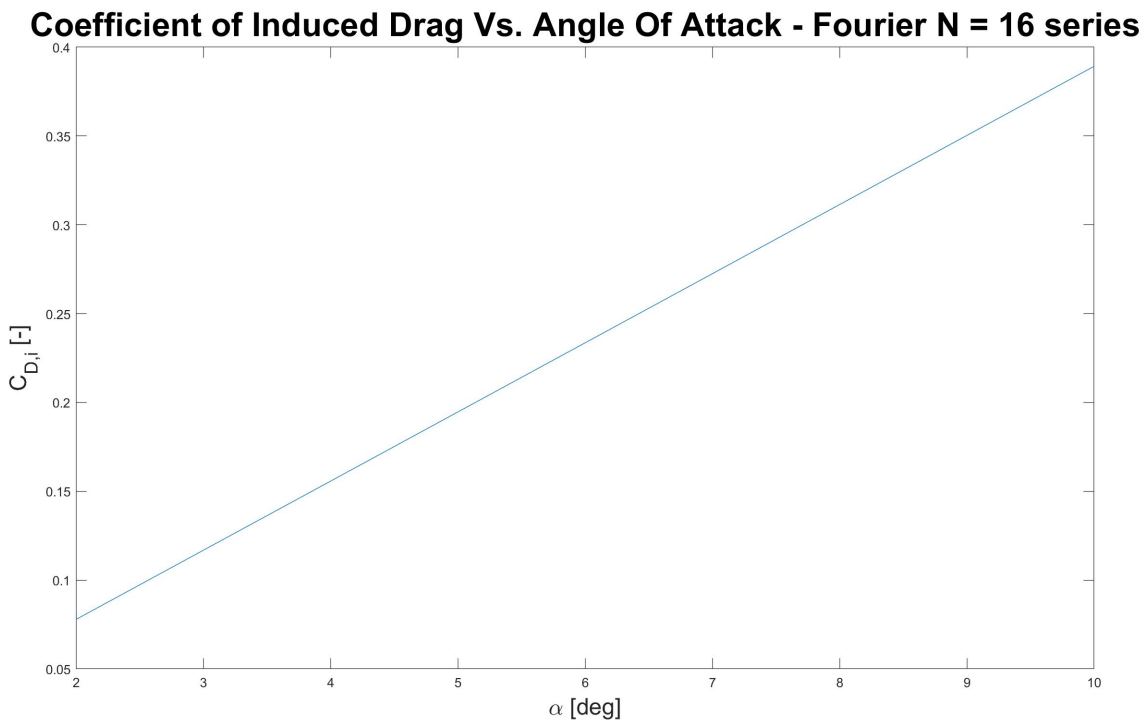

Figure 21: Coefficient of Drag vs. Angle of Attack for the Fourier N = 16 series for AR = 6

Interestingly enough, the drag followed a linear pattern unlike in the elliptical solution which was slightly non-linear.

2.3 Discussion

The elliptical and straight-blade wings compare very similarly. In fact, they predict almost the similar coefficient of lift. What is different, however, is their distribution of strength along the wing. For the elliptical method, there is a stronger distribution of circulation towards the edges. As the Fourier series expands, the distribution becomes almost constant throughout. Both end results end up with almost the same lift coefficient. However, for the drag coefficient, the results were quite different. The fourier solution was perfectly linear, despite being a function of CL^2, perhaps this could do with the fact that the elliptical solution does not have a factor in it. In fact, the book agrees with this. The minimum drag is yielded from the *elliptical lift distribution.* That is why there is a practical interest in the ellitpical lift distribution.

2.4 Taper Ratio

Unfortunately, I was not able to get the Taper Ratio to converge. The tapering should cause a decrease in drag and an increase in lift as discussed in the theory [2].

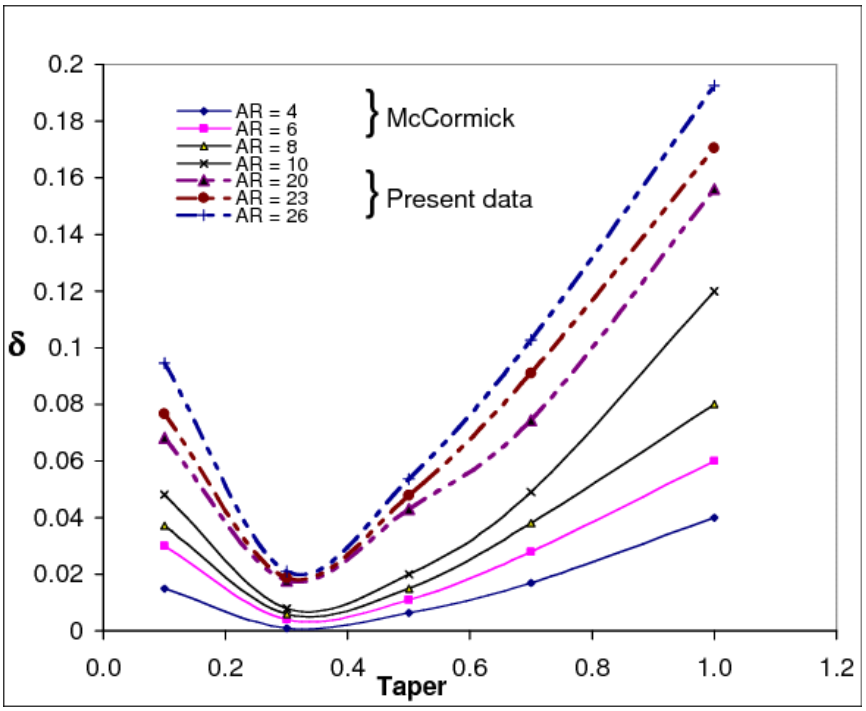

Figure 22: Induced Drag as a function of Taper From Research [5]

It seems that the theory is right - to a certain extent. Then, this pattern inverses. I researched some induced drag parameters versus taper that were published. This non-linear effect shows that as the tapering should cause a decrease in drag - to a certain extent. Also Aspect Ratio can play a role in increasing the drag. The drag coefficient also seems to have a minimum point around taper 0.3. Then, the drag will increase. So it seems that there is some optimization involved in this to maximize drag and lift effects that could be very interesting to study.

2.5 Effects of Aspect Ratio

Aspect Ratio affects both the fourier transform setup and the end multiplication in Equations 5.61 and 5.53 in the book [2]. Re-use the code from the subsection analysis 2.2 ending with AR =3,6,9,12 and plot the distribution of Cl vs α

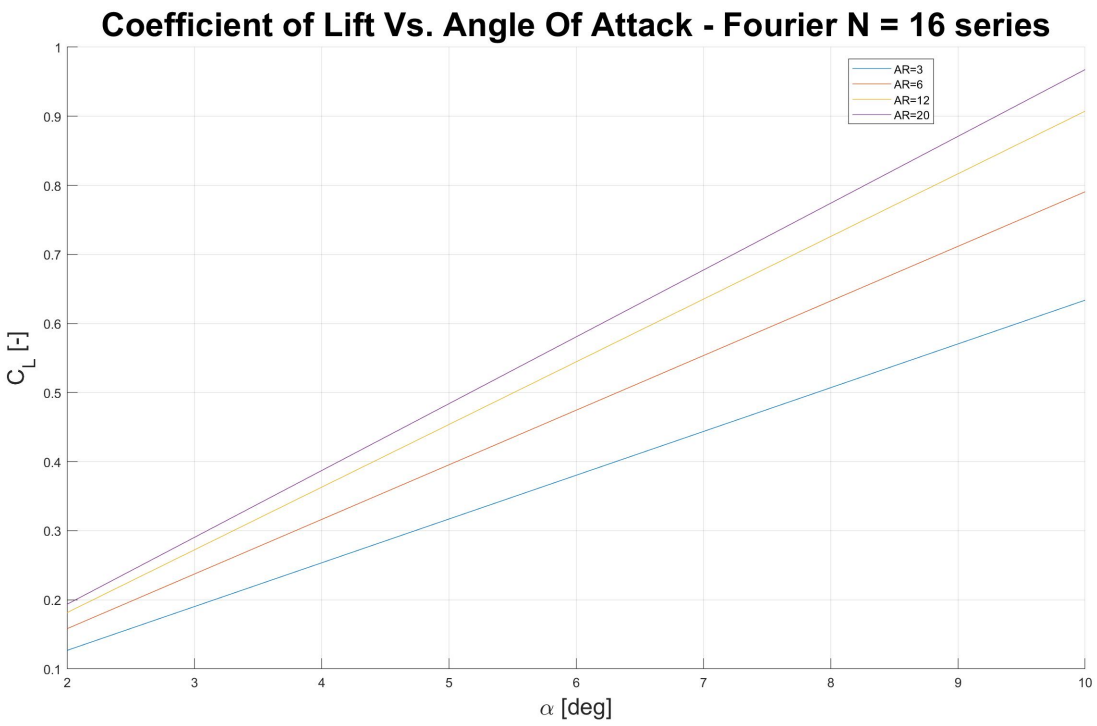

Figure 23: Coefficient of Lift vs. Angle of Attack for the Fourier N = 16 series for AR = 6

Overall, the Aspect Ratio seems to increase lift with decreasing margins. This makes sense because as AR –> ∞, then the wing is essentially becoming an infinite span wing rather than a finite span wing and the theory says that the infinite span wing would have a higher coefficient of lift.

3 Conclusion

In conclusion, there are many factors that go into airfoil theory. This report should give great insight to taper, aspect ratio, 3D airfoil distributions, and a great overview of 2D analysis in VP, Thin Airfoil, and XFLR data that a student coming into Aerodynamics could gain knowledge from.

References

[1] P. F. UW-Madison. (2022) In-class notes and lectures.

[2] J. Anderson, *Fundamentals of Aerodynamics, Sixth Edition*, 2017.

[3] M. Hepperle. Designing an airfoil. [Online]. Available: https://www.mh-aerotools.de/airfoils/methods.htm

[4] Ebrary. Panel method solvers - xfoil and xflr5. [Online]. Available: https://ebrary.net/59615/engineering/panel_method_solvers_xfoil_xflr5

[5] J. Katz. Aspect drag parameter versus taper ratio. [Online]. Available: https://www.researchgate.net/figure/nduced-drag-parameter-versus-taper-ratio-and-aspect-ratio-for-an-untwisted-rectangular_fig6_268564853